Available online at www.sciencedirect.com
ScienceDirect
Scripta Materialia 57 (2007) 413–416
Scripta MATERIALIA
www.elsevier.com/locate/scriptamat

Effect of non-linear liquidus and solidus in undercooled dendrite growth: A comparative study in Ni–0.7 at.% B and Ni–1 at.% Zr systems

Haifeng Wang, Feng Liu,* Zheng Chen, Wei Yang, Gencang Yang and Yaohe Zhou

State Key Laboratory of Solidification Processing, Northwestern Polytechnical University, Xi'an, Shaanxi 710072, China

Received 4 February 2007; revised 28 April 2007; accepted 30 April 2007
Available online 7 June 2007

A steady-state dendrite growth model proposed for binary alloys, which assumes non-linear liquidus and solidus, was used to compare dendrite growth in undercooled Ni–0.7 at.% B and Ni–1 at.% Zr alloys. In comparison with Ni–0.7 at.% B alloy, the effect of non-linear liquidus and solidus is strengthened in Ni–1 at.% Zr alloy, so that non-linear growth occurs at the so-called linear stage at high undercooling.

Keywords: Dendrite growth; Undercooling solidification; Non-linear; Rapid solidification; Alloy

The Lipton–Kurz–Trivedi (LKT)/Boettinger–Coriell–Trivedi (BCT) model [1,2] has become the most widely used model to predict dendrite growth in undercooled melts. However, many experiments have shown that the BCT model cannot be used to predict a deviation of growth mode from power law to linear growth above a critical undercooling ΔT^* [3–7]. Introducing a relaxation effect, i.e. non-equilibrium liquid diffusion [8–11], Galenko and Danilov [12,13] developed an original model that predicts the deviation from power law to linear growth. However, the above models, which assume linear liquidus and solidus, are generally only valid for small ΔT [14]. Assuming non-linear (NL) liquidus and solidus, a steady-state dendrite growth model was recently proposed [15] as an extension of Galenko and Danilov's model [12,13]. In the following, a concise description of the NL model is first given. In order to show the non-linear effect, a comparative study of undercooled dendrite growth between undercooled Ni–0.7 at.% B and Ni–1 at.% Zr alloys was performed applying the NL model [15], in combination with the phase diagrams of Ni–B (i.e. in which an assumption of linear liquidus and solidus is seemingly appropriate) and Ni–Zr (i.e. in which the liquidus and solidus are typically curved).

For a curved interface, assuming non-linear liquidus and solidus, a local interface curvature correction must be directly performed to derive the interfacial driving force ΔG from a planar interface [14]. As for the NL model, a summation of the above correction, the relaxation effect for a planar interface [16,17] and the linear kinetic law [18,19] leads to a corrected interface response function [15]

$$C_S^{eq}(T_i+\Delta T_R)-C_L^{eq}(T_i+\Delta T_R)+\frac{V}{V_0},\\ +C_L^*N(V,T_i+\Delta T_R)=0, \tag{1}$$

where

$$N(V,T_i+\Delta T_R)=1-k+\ln k/k'_e+\frac{V}{V_D}(1-k)^2,\quad V<V_D, \tag{2a}$$

$$N(V,T_i+\Delta T_R)=-\ln k'_e,\quad V\geqslant V_D, \tag{2b}$$

where $C_L^{eq'}=C_L^{eq}(T_i+\Delta T_R)$ and $C_S^{eq'}=C_S^{eq}(T_i+\Delta T_R)$ [14] with C_L^{eq} and C_S^{eq} as the equilibrium concentrations, C_L^* and C_S^* the non-equilibrium concentrations in liquid and solid, respectively, at the interface corresponding to the interface temperature T_i; V the interface velocity; V_0 the upper limit of the interface advancement; V_D the bulk liquid diffusion speed; $k=C_S^*/C_L^*$ and $k'_e=C_S^{eq'}/C_L^{eq'}$ the non-equilibrium and equilibrium partition coefficient subjected to the curvature correction; and ΔT_R

* Corresponding author. Tel.: +86 029 88460374; e-mail: liufeng@nwpu.edu.cn

1359-6462/$ - see front matter
doi:10.1016/j.scriptamat.2007.04.037

the curvature undercooling. Normally, the marginal stability criterion [20–23] is further combined to deduce a unique relation between V and ΔT. For the NL model, the marginal stability criterion from Eq. (1) with non-linear liquidus and solidus gives an expression for the dendrite tip radius R as [15]

$$R=\frac{\Gamma}{\sigma^*}\left(\frac{P_T\Delta H_f}{C_P}\xi_L+\frac{2M(V,T_i+\Delta T_R)P_C C_L^*(k-1)}{\psi}\xi_C\right)^{-1},\quad V<V_D, \tag{3a}$$

$$R=\frac{\Gamma}{\sigma^*}\left(\frac{P_T\Delta H_f}{C_P}\xi_L\right)^{-1},\quad V\geqslant V_D, \tag{3b}$$

where

$$\xi_C=1-\frac{2k+2M(V,T_i+\Delta T_R)C_L^*\partial k/\partial T|_{T=T_i+\Delta T_R}}{\sqrt{1+\psi(\sigma^*P_C^2)^{-1}}+2k-1+2M(V,T_i+\Delta T_R)C_L^*\partial k/\partial T|_{T=T_i+\Delta T_R}},\quad V<V_D \tag{4a}$$

$$\xi_C=0,\quad V\geqslant V_D, \tag{4b}$$

$$\xi_L=1-\frac{1}{\sqrt{1+(\sigma^*P_T^2)^{-1}}}, \tag{5}$$

$$M(V,T_i)=\frac{-m_L(T_i)m_S(T_i)N(V,T_i)}{m_L(T_i)-m_S(T_i)+m_L(T_i)m_S(T_i)C_L^*\partial N(V,T_i)/\partial T|_{T=T_i}}, \tag{6}$$

where Γ is the Gibbs–Thompson coefficient, ΔH_f the latent heat of fusion, $\sigma^*=1/4\pi^2$ the stability constant, $P_C=VR/2D$ the solutal Peclet number, $P_T=VR/2\alpha_L$ the thermal Peclet number, D the liquid diffusion coefficient, α_L the thermal diffusivity of liquid, C_P the specific liquid heat, m_L and m_S the slope of liquidus and solidus, and $\psi=1-V^2/V_D^2$. In contrast with previous models [2,12,13], Eq. (3a) implies that, for the NL model, both R and V are dependent on T_i for $V<V_D$.

Departing from solute-trapping model of Sobolev [9–11], which is an extension from Aziz's model [24,25], the non-equilibrium partition coefficient, for the NL model with curvature correction, can be given as [15]

$$k(V)=\frac{V/V_{DI}+k_e'\psi}{V/V_{DI}+\psi},\quad V<V_D, \tag{7a}$$

$$k(V)=1,\quad V\geqslant V_D, \tag{7b}$$

where V_{DI} is the interface diffusion speed.

Analogous to previous models assuming linear liquidus and solidus [2], the bath undercooling ΔT, for the NL model, also consists of four different terms [15], where $\Delta T_R=2\Gamma/R$ is the curvature undercooling, $\Delta T_T=\Delta H_f Iv(P_T)/C_P$ the thermal undercooling with $Iv(x)=x\exp(x)E_1(x)$ as the Ivantsov function [26,27], $\Delta T_C=T_L(C_0)-T_L(C_L^*)$ the constitutional undercooling, and $\Delta T_K=T_L(C_L^*)-T_L(C_L^{eq'})$ the kinetic undercooling. For a given ΔT, integration of Eqs. (1)–(7), uniquely, gives solutions for R and V. A detailed derivation of the NL model is available in Ref. [15].

Since non-linear liquidus and solidus are assumed in the NL model, the equilibrium partition coefficient k_e, the liquidus slope m_L, the interface response function (Eq. (1)) and the dendrite tip radius R (Eqs. (3a) and (3b)) must be obtained directly from the phase diagram, without any artificial adjustment [15]. It then follows that the NL model prediction is relatively physically realistic, while thermodynamic calculations of the phase diagram should be very accurate. Accordingly, the nickel-rich parts of the equilibrium Ni–B and Ni–Zr phase diagrams were precisely calculated using Thermo-Calc. The solidus and liquidus of the Ni–B phase diagram (Fig. 1a) change almost linearly as a function of temperature. However, the liquidus and solidus of the Ni–Zr phase diagram (Fig. 1b) deviate substantially from linearity, especially at low temperature. Therefore, a valid comparative study of the effect of the non-linear liquidus and solidus during undercooled dendrite growth can be conducted using these two alloy systems.

If linear liquidus and solidus are assumed, the NL model reduces to Galenko and Danilov's model, so it is meaningful to predict dendrite growth in undercooled Ni–0.7 at.% B and Ni–1 at.% Zr alloys using both models. The values of the parameters used are given in Table 1, and the other two specified parameters, i.e. $k_e=0.0155$ and $m_L=-14.3$ K/at.% [12] for Ni–0.7 at.% B alloy and $k_e=0.04$ and $m_L=-11$ K/at.% [7] for Ni–1 at.% Zr alloy, were adopted for Galenko and Danilov's model prediction. From Figure 2a and b, the NL model (solid line) gives a more satisfactory agreement with experimental data (open squares), in agreement with the corresponding discussion in Ref. [15]. In fact, for Ni–0.7 at.% B alloy, the Galenko–Danilov model prediction does not deviate much from the

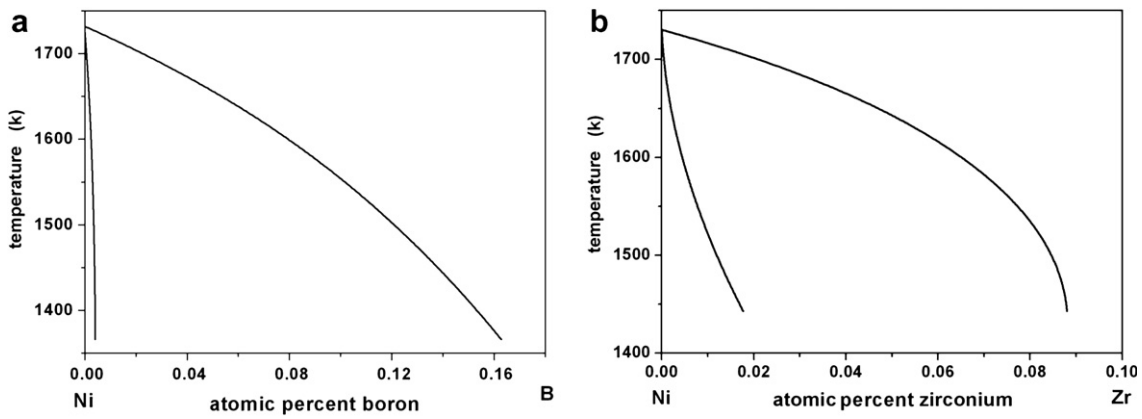

Figure 1. Equilibrium phase diagram obtained from Thermo-Calc for the nickel-rich part of (a) Ni–B and (b) Ni–Zr.